Improvement of Robustness in Blind Image Restoration Method Using Failing Detection Process

Takahiro Nagata and Tomio Goto
Dept. of Computer Science, Nagoya Institute of Technology, Nagoya, Japan
Email: yhr-0801@splab.nitech.ac.jp, t.goto@nitech.ac.jp

Satoshi Motohashi
Tokai Rika Co. Ltd., Toyota, Japan

Haifeng Chen and Reo Aoki
R&D, Visual Technologies (ASIC), EIZO Corporation, Ishikawa, Japan

***Abstract*—Blind image restoration, which restores a clear image from a single blurry image, is a difficult process of estimating two unknowns: a point-spread function (PSF) and an ideal image. In this paper, we propose a novel blind deconvolution method to alternately estimate a PSF and its latent image. We apply a gradient reliability map that enables edge selection appropriate for PSF estimation and an energy function that enables estimation of convergence states. This method improves restoration performance by eliminating noise adversely affecting estimation. Additionally, a restoration failure detection process is added by using an evaluation function. Experimental results show that the robustness of the proposed method is improved and high quality images are obtained.**

***Index Terms*—blur, blind deconvolution, image restoration, point spread function**

I. Introduction

Currently, smart phones and social network services (SNS) have been being widely used by consumers. Furthermore, it is very easy to take photos at any time. Unfortunately, many of those pictures suffer from image blurring because of photo dynamics, such as shaky cameras and poor focus. Furthermore, image blurring cannot be easily detected on small displays of most devices. However, image blurring can be recognized on larger displays, such as High-Definition Televisions (HDTV) and laptops. This type of degradation is visually undesirable, and restoration of the degraded image is required.

Blur is an example of image deterioration, and many studies on image restoration have been proposed [1]-[6]. In the case of restoring a degraded image, when a blurring function is unknown, it becomes necessary to estimate a Point Spread Function (PSF) and its ideal image by using an input image. A method of alternately repeating PSF and ideal image estimations produces good results. However, there are some problems such as the occurrence of ringing caused PSF estimation errors and noise emphasis. Therefore, further improvements in restoration performance are required. In this paper, a novel algorithm based on a blind two-step deconvolution is proposed. In our proposed method, during the latent image restoration step, total variation regularization [7], [8] is applied to reduce texture components and noise. A shock filter [9]-[10] is applied to emphasize edges, resulting in improvements to the PSF estimation performance. The method of Krishnan *et al.*, which offers fast processing, is implemented at deconvolution processes, enables high-speed processing. The gradient reliability map is then applied to decrease edges, which are badly affected during PSF estimation, further improving performance. This is our main proposal, in contrast to our conventional work [5]. Additionally, an energy function is applied to the ideal image estimation process to detect restoration failure. In our experiments, the parameters for the threshold process of the gradient distributions are first optimized to improve restoration performance. Then, Sun's test set [3] is used to validate our proposed method in objective evaluations. Finally, actual blurred images are used to evaluate our proposed method objectively and subjectively.

II. Image Restration Algorithm

When image blurring in an image is uniform, blurred image b is modeled as the convolution of latent image x and its PSF k as follows, where n is noise.

$$b = x \otimes k + n \quad (1)$$

In this paper, we restore images using this blur degradation model. Image restoration can be classified as non-blind or blind deconvolution. Non-blind deconvolution is image restoration when a PSF is known, and blind deconvolution is image restoration when a PSF

Manuscript received December 19, 2018; revised March 13, 2019.

doi: 10.18178/joig.7.1.1-8

is unknown. Blind deconvolution is a problem of estimating both an ideal image and its PSF from a single degraded image. Generally, we estimate the final PSF by alternately repeating the latent image estimation (x-step) and its PSF counterpart (k-step). We restore the degraded image by performing a final non-blind deconvolution using the estimated PSF.

III. Blind Image Restoration

Blind image reconstruction is a problem of estimating an ideal image and a degraded PSF from single degraded image. In general, it solves the problem of restoring the ideal image from the estimated PSF (x-step) and the problem of estimating PSF from degraded image (k-step), and performs image restoration by alternately performing these steps. The flow of the blind image restoration is shown in Fig. 1.

In our proposed system,, x-step is composed of three stages of deconvolution, TV regularization, and Shock Filter. In addition, k-step performs processing by the differentiation of degraded image, differential and threshold processing of estimated imaginary image, and PSF calculation by conjugate gradient method. Also, in order to cope with large blur, we use multiscale iterative processing like Cho's method [1]. As a flow of this process, the image size is first reduced, and x-step and k-step are alternately repeated while gradually expanding to the original size, and the PSF estimation is repeated for each scale. The initial value of PSF uses 3 × 3 Gaussian filter. In addition, alternate iterative processing of PSF estimation is done in gray scale. Then, the final deconvolution is performed using the PSF finally obtained by the iterative process.

A. *Latent Image Estimation (x-step)*

In the x-step, first, a restored image x is obtained by deconvolution. However, since noise and ringing occur in the restored image, the texture component of the restored image is removed by TV regularization. Then, a shock filter is applied to the obtained structure component to restore the edge included in the structure component of the image, thereby estimating the ideal image x.

1) *Deconvolution*

Restore the ideal image x using PSF k obtained by PSF estimation processing. In this research, we use high speed deconvolution using hyper-Laplacian priors proposed by Krishnan *et al.* [11] This method uses statistical knowledge that the gradient histogram of a natural image obeys a distribution called a heavy tail, and solves the minimization problem of (2) to find an ideal image x. Latent image x is determined by solving the following minimization problem.

$$\mathrm{x} = min_x \sum_{i=1}^{N} \left(\frac{\lambda}{2} (x \otimes k - b)_i^2 + \sum_{j=1}^{J} \left| (x \otimes d_j)_i \right|^2 \right) \tag{2}$$

where d is a differential filter and $|.|^2$ is a penalty function.

2) *Total variation regularization*

Total variation regularization [7] is often used to decompose an image into a structure component, which consists of edges and low-frequency components; and a texture component, which consists of small oscillating signals and noise. In the ROF model [7], the evaluation function $F(u)$ is minimized to solve an image decomposition as shown in (3):

$$\inf_u F(u) = \sum_{i,j} \left|\nabla_{i,j}\right| + \lambda \sum_{i,j} \left|u_{i,j} - f_{i,j}\right|^2 \tag{3}$$

where $f_{i,j}$ is an input pixel value, $u_{i,j}$ is a computed output pixel value, i and j are pixel coordinates, and λ is a positive constant. To minimize the evaluation function $F(u)$, we adopt the projection method proposed by Chambolle [8], which is known to be a fast solution. The values, u and $v = f - u$, are the structure and texture components, respectively. The projection method of Chambolle [8] can be expressed by (4) and (5). Where g is an input image, f is an output image, λ is a regularization parameter, τ is a step width, and $p_{x,y}^{(0)} = 0$.

$$p_{x,y}^{(i+1)} = \frac{p_{x,y}^{(i)} + \tau\left\{\nabla\left(\mathrm{div}p_{x,y}^{(i)} - g/\lambda\right)\right\}_{x,y}}{1 + \tau\left|\nabla\left(\mathrm{div}p_{x,y}^{(i)} - g/\lambda\right)_{x,y}\right|} \tag{4}$$

$$f = g - \lambda \mathrm{div}p_{x,y}^{(i+1)} \tag{5}$$

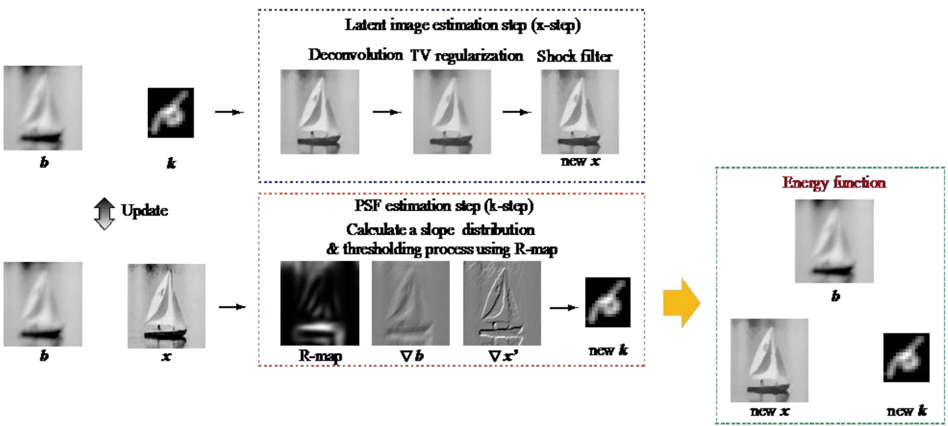

Figure 1. Processing flow of our proposed blind deconvolution

3) Shock filter

The shock filter [9], [10] is a filter, which was proposed by Osher and Rudin, that restores or emphasizes edges of an input signal by iterative calculation. The shock filter is represented by the following (6).

$$x_{t+1} = x_t - \mathrm{sign}(\Delta x_t)\|\nabla x_t\|dt \tag{6}$$

where dt is the step-size parameter for the shock filter. The shock filter can adjust the convergence speed according to the value of the step-size dt, and if the dt is 1 or less, it is a filter that can emphasize the edge without causing ringing.

B. PSF Estimation (k-step)

During the k-step, we perform a thresholding process to obtain latent image x estimated during the x-step and to estimate PSF k by solving a minimization problem using a degraded image b and an ideal image x. One specific method for thresholding is dividing the directions of the gradient into four groups: 0°, 45°, 90°, and 135°. We then set the threshold α_g, which is a coefficient of several pixels selected for each group. During the PSF estimation, by using observed image gradient distribution ∇b and predicted latent image gradient distribution ∇x, PSF k is estimated. By minimizing the conjugate gradient method of an energy function as shown in (7), PSF k is estimated thusly.

$$E_k(k) = \left\|\nabla x' \otimes k - \nabla b\right\|^2 + \lambda_k\|k\|^2 \tag{7}$$

IV. Proposed Method

Blind deconvolution occasionally causes a PSF estimation error because of its fine texture components. This may result in failure to restore images. To further improve the restoration performance of blind deconvolution, we add a new process called the "energy function" to the k-step. The energy function represents the degree of convergence of the PSF. Fig. 1 shows the processing flow of the proposed method. Furthermore, if a failure occurs during the iterative process, failure detection is needed to prevent an adverse effect after the iteration, provided there is no breakdown prevention.

A. Gradient Reliability Map (R-map)

During the minimization problem for the PSF estimation of our proposed method, strong edges are used. However, those may have a negative influence, owing to noise or narrow signals such as impulse signals. A narrow signal, which is narrower than the blur size, causes a smaller amplitude value when the shock filter emphasizes its edge. This results in an incorrect estimation. Therefore, we apply the gradient reliability map (i.e., R-map) as shown in (8), where $N_h(x)$ is an $h \times h$ window at the center position x. Fig. 2 shows an example of an R-map.

$$r(x) = \frac{\left\|\sum_{y \in N_{h(x)}} \nabla b(y)\right\|}{\sum_{y \in N_{h(x)}} \|\nabla b(y)\| + 0.5} \tag{8}$$

In (8), a thin signal is a numerator with plus and minus cancellation, and r is small. Also, in the flat region, r decreases with the denominator of 0.5. Therefore, if r is large, the reliability of the gradient is high. This r becomes the gradient reliability map (R-map) as it is. Then, a thin signal is excluded by multiplying r' after binarization of r by the gradient of the estimated ideal image. After that, gradient distribution threshold processing is performed. It can be confirmed that the character portion which is one of the thin signals in the deteriorated image is excluded by the gradient reliability map.

(a) Burred image (b) R-map

Figure 2. Example of a gradient reliability map

B. Energy Function

We propose a method of calculating the energy value from the difference between the estimated blur-degraded image and the input image as an index for detecting failure [12]. According to the calculation formula of (9), the difference of the blur-deteriorated image is calculated by the brightness value, and the sum of the squares of the absolute value is taken as the main value of energy. As the energy value decreases, the objective function converges, which means that the restoration succeeds.

$$e = \frac{|b - x * k|^2}{w * h} \tag{9}$$

where, b is an input blurred image, x is an estimated ideal image, k is an estimated PSF, and $x * k$ is an estimated blurred image. Also, w and h are the vertical and horizontal sizes of the image, and the energy value is normalized by dividing by the total number of pixels. As a calculation, the difference between the estimated blurring degraded image and the blurred degraded image at the input is calculated with the luminance value, and the energy value is calculated from the square sum of the absolute values. As the energy value decreases, the objective function of the blind deconvolution converges, so it can be confirmed that the restoration is going to be successful. Fig. 3 shows the actual values used for calculation. When the PSF estimation fails, it can be confirmed that the difference between the estimated blurred degraded image and the input blurred degraded image has a value.

(a)b (b) $x * k$

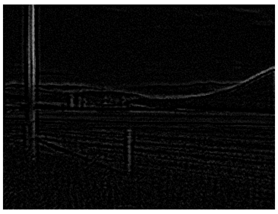

(c) $|b - x * k|$

Figure 3. Visualization image of energy value

C. Corruption Detection Processing

In our proposed method, after processing at the x- and k-steps, based on the method of previous research [13], the energy value is used as a breakdown detection process regarding the energy value. As an example of the energy transition diagram, an energy transition diagram at the time of successful restoration is shown as Fig. 4(a), and an energy transition diagram at the time of failure recovery is shown in Fig. 4(b). From the results of the energy transition diagram, it can be seen that the energy transition of the image successfully restored in Fig. 4(a) converges with each iteration of processing. On the other hand, it can be confirmed that the energy transition of the image failing to restore in Fig. 4(b) tends to be in an unstable state without converging by iteration. Therefore, the energy values are compared before and after the iterative process, and when the energy decreases, the recovery is regarded as being successful and the estimated PSF is updated. Conversely, when the energy increases, it is considered that the restoration has failed, and the one that the estimated PSF is currently obtained is used for the next iterative process. Further, when it is regarded as a restoration failure, it is conceivable that the subsequent PSF estimation also fails, so the threshold parameter of the PSF estimation is changed. By setting the threshold value to a large value, spreading of the PSF that is confirmed at the time of PSF estimation error is suppressed and prevention of collapse is prevented. However, when the image size is increased by multiscale processing, the tendency of the energy value to increase in many images has been confirmed, so failure detection processing is not executed only at that time.

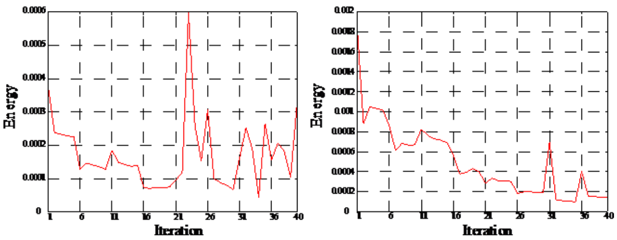

(a) Restore success example (b) Restore failure example

Figure 4. Example of energy transition diagram

V. Experimental Results

A. Objective Evaluation Experiment with Sun's Test Set

In this section, we perform evaluation experiments using the test image set [3] for evaluating blurred image restoration proposed by Sun *et al.* In the evaluation using Sun's test set, 640 degraded images are restored, error rate, PSNR and success rate are calculated and these are used as evaluation values. This evaluation method has been adopted in many articles in recent years. In the experiments in this section, we compare our proposed method with the related research method [1, 2, 3, 4 and 5]. Also, in this evaluation, the final non-blind deconvolution is unified into Zoran's method [14], so that it focuses only on PSF estimation. In this evaluation, the PSNR of the ideal image and the restored image is measured. Furthermore, the error rate r indicated by (10) is also measured.

$$r = \frac{\|x - \hat{x}_{\hat{k}}\|^2}{\|x - \hat{x}_k\|^2} \tag{10}$$

where x is an ideal image, and $\hat{x}_{\hat{k}}$ is a restored image using the estimated PSF of each method. Also, $\hat{x}_k$ is a restored image using the ideal PSF. As the error rate r approaches 1, it is a better result. Table I shows experimental conditions of our proposed method. For α_g, optimized values are used. The results of the objective evaluation are shown in Table II, and the cumulative error rate showing the success rate is shown in Fig. 5. Here, the average PSNR and the average error rate are the average of the experimental results of 640 sheets, and the maximum error rate shows the error rate of the image with the worst restoration result. Also, regarding the success rate, it shows the ratio of the image with an error rate of 5 or less. In this experiment, if the error rate is less than 5, it is evaluated in Michaeli *et al.* [4] that the restoration was successful, and the same evaluation is done in this paper. In Table II, our proposed method has better evaluation values at the maximum error rate than the conventional method. When comparing the results of the average PSNR, average error rate, and maximum error rate, the proposed method has a somewhat lower value than the conventional method. However, compared with other researchers' restoration methods, it was confirmed that they showed high recovery performance.

In other words, it can be confirmed that our proposed method is a method to prevent significant degradation while maintaining the conventional restoration performance. However, when comparing the method of Michaeli *et al.* with the maximum error rate, it can be confirmed that there is still a big difference. This is because our proposed method does not succeed in restoring with all of the images that failed in the conventional method, and part of the restored original image that remained in failure was left. On the other hand, the method by Michaeli *et al.* has no major breakdown, which shows that it is a stable method for all images. In addition, as shown in Fig. 6, our proposed method has fewer high-definition images with lower error rates than the conventional method, and few images with large error rates of 10 or more are obtained. On the other hand, when compared with the method by Michaeli *et al.*, there are some high-definition images, and some images that failed largely are also obtained. From this, it can be confirmed that our proposed method is obtained a fine resolution and a robust restoration method with characteristics of both the conventional method and Michaeli's method.

TABLE I. EXPERIMENTAL PARAMETERS FOR PROPOSED METHOD

PSF size			31 × 31
Iterative number at each scale			5
Latent image estimation process	Deconvolution	λ_d	1500
	TV Regularization	Iterative number	10
		λ_d	20
	Shock Filter	Iterative number	1
		dt	1.0
PSF estimation process	Iterative number		30
	Threshold value		0.05
	α_g		45

TABLE II. EXPERIMENTAL RESULTS OF OBJECTIVE EVALUATIONS

Methods	Average PSNR [dB]	Average Error Ratio	Max Error Ratio	Success Rates [%] ($r \leqq 5$)
Blur input	24.62	6.86	25.92	35.63
Known PSF	32.33	1.00	1.00	100.00
Cho & Lee [1]	26.65	9.00	118.28	68.26
Xu & Jia [2]	29.19	3.08	65.36	88.63
Sun *et al.* [3]	30.20	2.14	24.98	93.71
Michaeli & Irani [4]	29.06	2.38	**9.23**	95.47
Conventional method [5]	30.21	2.23	48.39	93.44
Proposed method	**30.87**	**1.64**	24.13	**96.72**

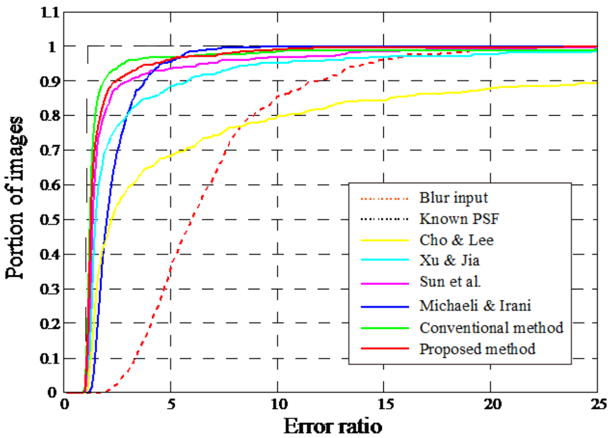

Figure 5. Experimental results of cumulative error rate

Fig. 6 and Fig. 7 show examples improved by the proposed method, and Fig. 8 and Fig. 9 show examples degraded by the proposed method. Fig. 10 and Fig. 11 show the energy transition diagram. In Fig. 6, whereas the restoration result is improved by using our proposed method. This image was difficult to restore by conventional methods, and some ringing near the white line of the road can be seen. This result as shown in Fig. 7 shows that the proposed method approaches the ideal PSF compared to the conventional method. However, the lateral PSF widening effect of the shape remains. By comparing the energy transition in Fig. 10, the value that violently fluctuates by the conventional method converges considerably stably by the proposed method. Thus, it is possible to confirm a clear difference in the result. In Fig. 8, the restoration result is improved by the proposed method, whereas the restoration fails by the conventional method. Moreover, in Fig. 9, the extra shape spread of the estimated conventional PSF has been removed by the proposed method. This can be estimate as a simple form close to the ideal PSF. Additionally, in Fig. 11, when comparing the energy transition of the conventional and the proposed methods, the proposed method loses significant fluctuations at the second half of the restoration in iterative process. It also confirms a stable transition and is thought to lead to a successful restoration. In the experimental results, the restoration succeeded in several images, which failed with the conventional method. Additionally, in our proposed method, it is difficult to cause failures.

In Table II, since Michaeli's method shows high performance from the viewpoint of the maximum error rate, pursuit of further robustness of the proposed method is an issue for further research.

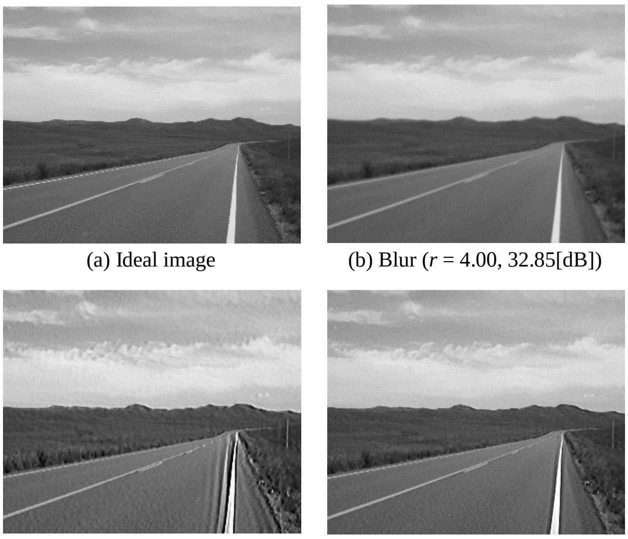

(a) Ideal image (b) Blur (r = 4.00, 32.85[dB])

(c) Conventional method [5] (r = 23.04, 24.72 [dB]) (d) Proposed method (r = 4.85, 31.83 [dB])

Figure 6. Blurred image and restored images (Road image)

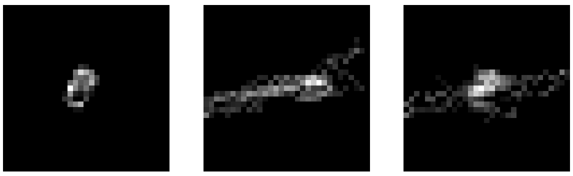

(a) Ideal PSF (b) Conventional method [5] (c) Proposed method

Figure 7. Estimated PSFs (Road image)

(a) Ideal image (b) Blur (r = 4.77, 28.75[dB])

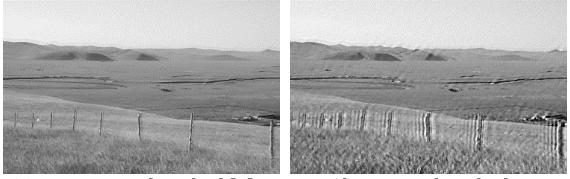

(c) Conventional method [5] (r = 10.45, 24.81[dB])　(d) Proposed method (r = 1.68, 33.32[dB])

Figure 8. Blurred image and restored images (Prairie image)

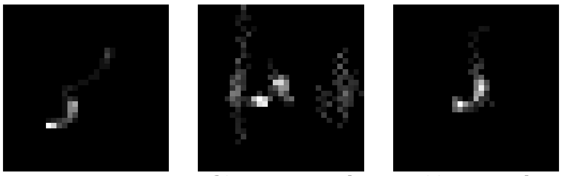

(a) Ideal PSF　(b) Conventional method [5]　(c) Proposed method

Figure 9. Estimated PSFs (Prairie image)

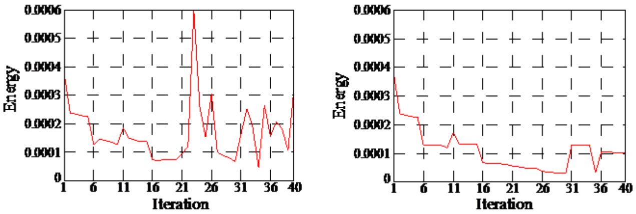

(a) Conventional method [5]　(b) Proposed method

Figure 10. Comparison of energy transition (Road image)

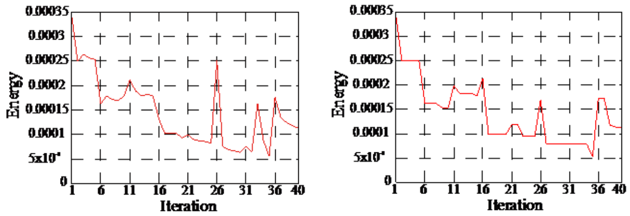

(a) Conventional method [5]　(b) Proposed method

Figure 11. Comparison of energy transition (Prairie image)

B. *Experiment on Degraded Images Actually Taken*

In this section, experiments are carried out on actual shake images, and compared with the methods of the conventional method [12] and Michaeli *et al.* [4], we verify the practicality of our proposed method in terms of both restoration performance and processing time. Experimental conditions are shown in Table III, degraded images, restored images and estimated PSFs are shown in Fig. 12 to Fig. 20. We cite Lyndsey image, Wall image and Postcard image from the reference [3], [2] and [15], respectively. The final deconvolution is unified by the fast Krishnan method [11]. First, the restoration results of Lyndsey images are compared. In Fig. 12, all restoration results of Michaeli's method, the conventional method, and our proposed method are sharper than the degraded image. In Fig. 13, it is confirmed that the same PSF is obtained for the conventional method and the proposed method, and the same result is obtained for the restored images. In addition, it can be confirmed that both the conventional method and the proposed method have better results than Michaeli *et al.* method compared with the enlarged view in Fig. 14. Next, the restoration results of the Wall image are compared. In Fig. 15, it is impossible to completely eliminate the blur deterioration, but good restoration results are obtained by the conventional method and the proposed method. In the comparison in Fig. 16, the PSF of the approximate shape can be estimated by the conventional method and the proposed method, but in Michaeli *et al.* method, since only a few blurs could be estimated, it is considered that the blurring deterioration remained. In addition, in Michaeli *et al.* method in Fig. 17, almost the same result as the input degraded image is obtained, and the restoration has failed. Finally, compare the restoration results of the Postcard image. In Fig. 18, it can be confirmed that a clear restoration result is obtained by our proposed method. In the conventional method and Michaeli *et al.* method, the restoration failed, and most of the blur remained. Even in the case of comparison with the enlarged view in Fig. 20, the blurring removal effect is seen in our proposed method in the surroundings of characters which could not be confirmed in other methods, and it is very clear. Also from the results of the estimated PSF in Fig. 19, the trajectory representing the blur is found in the proposed method, whereas the other methods gather at one point, failing to estimate the shake. However, when restoring images with large blur such as Postcard images, there is a tendency to fail to estimate, so further study on a more robust restoration method for photographed images is a future task. Also, comparison of the processing time is performed for three real-life deteriorated images. As a result, the conventional method and the proposed method were about the same degree. In the proposed method and Michaeri's method, the proposed method was over 100 times faster.

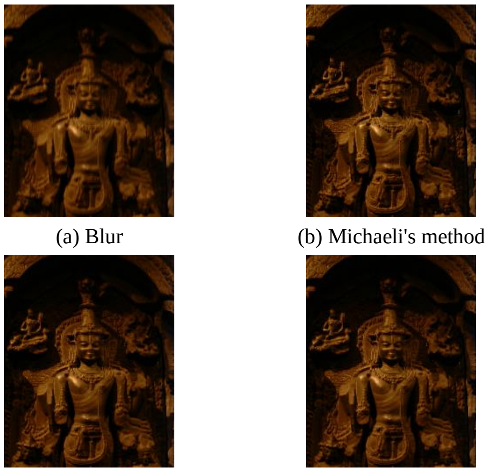

(a) Blur　(b) Michaeli's method　(c) Conventional method [5]　(d) Proposed method

Figure 12. Real image restoration result (Overall: Lyndsey)

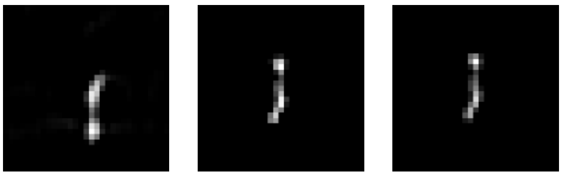

(a) Michaeli's method　(b) Conventional method [5]　(c) Proposed method

Figure 13. Estimated PSFs (Lyndsey)

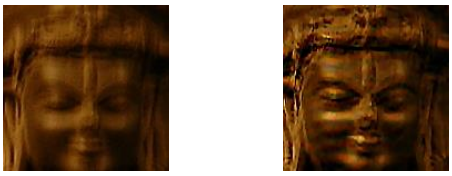

(a) Blur (b) Michaeli's method

(c) Conventional method [5] (d) Proposed method

Figure 14. Real image restoration result (Enlarged : Lyndsey)

(a) Blur (b) Michaeli's method

(c) Conventional method [5] (d) Proposed method

Figure 15. Real image restoration result (Overall: Wall)

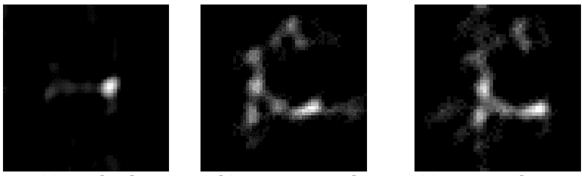

(a) Michaeli's method (b) Conventional method [5] (c) Proposed method

Figure 16. Estimated PSFs (Wall)

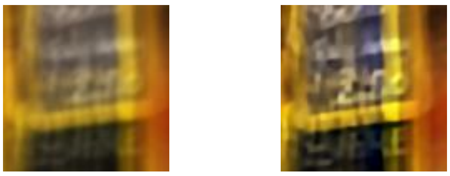

(a)Blur (b) Michaeli's method

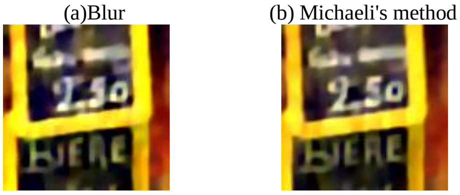

(c) Conventional method [5] (d) Proposed method

Figure 17. Real image restoration result (Enlarged: Wall)

(a)Blur (b) Michaeli's method

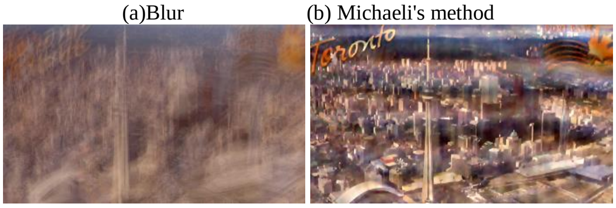

(c) Conventional method [5] (d) Proposed method

Figure 18. Real image restoration result (Overall: Postcard)

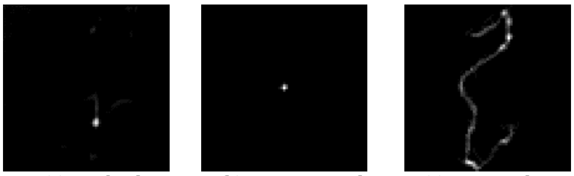

(a) Michaeli's method (b) Conventional method [5] (c) Proposed method

Figure 19. Estimated PSFs (Postcard)

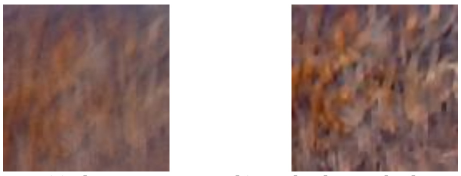

(a)Blur (b) Michaeli's method

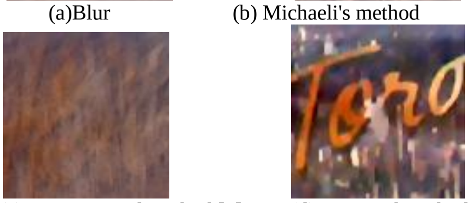

(c) Conventional method [5] (d) Proposed method

Figure 20. Real image restoration result (Enlarged: Postcard)

TABLE III. EXPERIMENTAL IMAGE AND PSF SIZE

Experiment image	Lyndsey	Wall	Postcard
Image size	724 × 905	436 × 511	728 × 470
PSF size	31 × 31	51 × 51	71 × 71

VI. CONCLUSION

In this paper, we have proposed a robust reconstruction method that succeeded with blur function estimation by adding corruption detection processing using an energy function. Experimental results have showed that the proposed method obtained better evaluation values than the conventional method and other related research methods. Also, in experiments using actual blurred images, we confirmed that the proposed method is effective to some extent in real images. In the objective evaluations, the maximum error rate was much higher than the other methods, and the proposed method was a robust restoration method that hardly caused a large collapse, but instead maintained high restoration performance of the conventional method. And the evaluation value of the maximum error rate for our proposed method was higher than that of Michaeli *et al.* method and lower than that of the conventional method. Thus, the overall restoration performance was much higher than that of the conventional method, because the threshold parameter in the PSF estimation process could be changed by adding the failure detection to our proposed method. Therefore, the fine-estimated PSF and the restored ideal image were obtained. This was difficult with the conventional method. Whereas the energy value decreased in calculation, the shape of the estimated PSF did not accurately represent some cases. Additionally, in the experimental results, it was very difficult to detect complete failure with the current method. Therefore, for further research, we intend to improve robustness while maintaining restoration performance. As a failure detection method, a method to improve the current failure detection by adding a regularization term to the energy value, methods for detecting failure from the shape of the estimated PSF, or adding a new constraint to the estimated PSF will be required. In recent years, learning type restoration methods such as deep learning and neural network are actively carried out in blind deconvolution, and by using such processing in PSF estimation, further improvement for restoration performance is expected. In addition, blind deconvolution may succeed or fail to restore by changing the parameters, and some of the blind deconvolution has high sensitivity of restoration parameters depending on input images and those PSFs. Therefore, if we can change the parameters according to the characteristics of them, we can realize further improvement for restoration performance and robustness.

Acknowledgment

This work was supported by JSPS KAKENHI Grant Number JP18K11372.

References

[1] S. Cho and S. Lee, "Fast motion deblurring," *Transactions on Graphics (SIGGRAPH)*, vol. 28, no. 5, pp. 1-8, 2009.

[2] L. Xu and J. Jia, "Two-Phase kernel estimation for robust motion deblurring," in *Proc. European Conference on Computer Vision*, Sep. 2010, pp. 57-170.

[3] S. Cho, L. Sun, and J. Wang, "Edge-Based blur kernel estimation using patch priors," in *Proc. IIEEE International Conference on Computational Photography*, 2013, pp. 1-8.

[4] T. Michaeli and M. Irani, "Blind deblurring using internal patch recurrence," in *Proc. European Conference on Computer Vision*, Sep. 2014, pp. 783-798.

[5] K. Ohkoshi, T. Goto, S. Hirano, and M. Sakurai, "Blind image restoration based on total variation regularization and shock filter for blurred images," in *Proc. IEEE Global Conference on Consumer Electronics*, 2014, pp. 219-220.

[6] S. Liu, H. Wang, J. Wang, S. Cho, and C. Pan, "Automatic blur-kernel-size estimation for motion deblurring," *The Visual Computer*, vol. 31, no. 5, pp. 733–746, 2015.

[7] S. J. Osher and E. Fatemi, "Nonlinear total variation based noise removal algorithms," *Physica D*, vol. 60, pp. 259-268, 1992.

[8] A. Chambolle, "An algorithm for total variation minimization and applications," *Journal of Mathematical Imaging and Vision*, vol. 20, no. 1, pp. 89-97, 2004.

[9] S. J. Osher and L. I. Rudin, "Feature-Oriented image enhancement using shock filters," *SIAM Journal on Numerical Analysis*, vol. 27, pp. 910-940, 1990.

[10] J. G. M. Schavemaker, M. J. T. Reinders, J. J. Gerbrands, and E. Backer, "Image sharpening by morphological filtering," *Elsevier Pattern Recognition*, vol. 33, no. 6, pp. 997-1012, Jun. 2000.

[11] D. Krishnan and R. Fergus, "Fast image deconvolution using hyper-Laplacian prior," in *Proc. Neural Information Processing Systems*, Dec. 2009, pp. 1033-1041.

[12] S. Cho and S. Lee, "Convergence analysis of MAP based blur kernel estimation," in *Proc. International Conference on Computer Vision*, 2017, pp. 4808-4816.

[13] S. Motohashi, T. Nagata, T. Goto, R. Aoki, and H. Chen, "A study on blind image restoration of blurred images using R-map," in *Proc. International Workshop on Advanced Image Technology*, 2018, no. 35.

[14] D. Zoran and Y. Weiss, "From learning models of natural image patches to whole image restoration," in *Proc. IEEE International Conference on Computer Vision*, 2017, pp. 479-486.

[15] W. Lai, J. Ding, Y. Lin, and Y. Chuang, "Blur kernel estimation using normalized color-line priors," in *Proc. International Conference on Computer Vision and Pattern Recognition*, 2015, pp. 64-72.

Takahiro Nagata received the B.S. degree from the Department of Electrical and Electronic Engineering, Nagoya Institute of Technology, in 2017. He is currently pursuing the M.S. degree from the Department of Computer Science, Nagoya Institute of Technology, Japan. His research interests are signal and image processing and blind image restration.

Tomio Goto (M'01) received the B.S., M.S., and Ph.D. degrees from Nagoya Institute of Technology in 1997, 1999, and 2007, respectively. He is currently an associate professor with the Department of Computer Science, Nagoya Institute of Technology, Japan. His research interests include coding of images, non-linear filtering, noise reduction, and super-resolution, as well as most other applications of digital image processing. He is a senior member of the IEEE, IEICE, ITE, and IEEJ in Japan.

Reo Aoki was born in Gifu, Japan, on Jun 28, 1981. He received the B.E. from Tokyo Metropolitan Institute of Technology in 2004, and M.S. from Japan Advanced Institute of Technology in 2006. Since 2006, He has been in EIZO Corporation, Hakusan, Japan. His research interests include video/image processing.

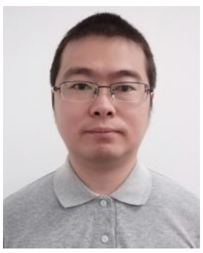

Haifeng Chen received the B.E. degree from East China University of Science and Technology, China, in 2002, and the M.S. degree from Shanghai Jiao Tong University, China, in 2005. Since 2005, he has been in EIZO Corporation, Hakusan, Japan. His research interests include video/image processing.